INJURY BIOMECHANICS RESEARCH
Proceedings of the Forty Third International Workshop

Measurement of Head Kinematics in Impact Conditions Using a Coplanar 6aω Configuration

Y. Kang, S. Goldman, K. Moorhouse and J. Bolte

ABSTRACT

The capability of accurately measuring the head kinematics in motor vehicle crash conditions is important for assessing brain injuries as well as head-neck loads and kinematics often associated with whiplash-like injuries in rear impacts. In this study, a coplanar configuration using six accelerometers and three angular rate sensors (ARS) was proposed and tested for the purposes of measuring accurate 6 degrees of freedom (DOF) kinematics in high-magnitude head impacts. The benefits of this configuration are its ability to minimize the use of error-producing numerical methods, such as numerical integration and differentiation, often found in traditional sensor configurations. The newly designed coplanar 6aω fixture (c6aω) was placed at the center of gravity of a Hybrid III ATD head. Similarly, nine accelerometers installed on a previously validated tetrahedron fixture (tNAAP) were placed on the skull cap of the Hybrid III ATD head for direct comparison during severe impact scenarios. The head-neck apparatus was impacted at various high speeds and directions by a pneumatic ram with a mass of 23.9 kg. These tests were conducted with the neck secured to a fixed surface as well as a surface that was free to slide in the direction of the ram impact. Three different impact directions were used in each scenario. For the fixed neck trials, the impact velocities were 1.5m/s, 2.5m/s, and 3.0m/s, while for the slide trials, the impact velocities were 1.5m/s, 2.5m/s, 3.0m/s, and 3.5m/s. All combinations of neck fixture, angle, and impact speed were repeated three times for a total of 63 tests. Normalized root-mean-square deviation (NRMSD) values and peak differences for both linear and angular acceleration were used for comparison. Both the average NRMSD and peak differences between the linear and angular acceleration calculated from the c6aω configuration and those from the tNAAP was less than 5% for all impact scenarios, indicating that the two configurations are equally capable of measuring angular accelerations. Furthermore, the c6aω configuration should provide improved measurement of angular velocity and rotation over tNAAP, so this instrumentation technique should be able to provide accurate comprehensive 6DOF kinematics for assessing TBI and neck injuries in future tests.

INTRODUCTION

Every year, nearly 1.5 million American citizens suffer a traumatic brain injury (TBI) due to events ranging from falls and automobile crashes to recreational sports injuries (Uhl et al., 2013). Furthermore, TBI was found to be the leading cause of death for passengers aged 5-24 in motor vehicle crash scenarios (Faul et al., 2010). The danger of TBIs can be partially attributed to their ability to remain "silent", as there are no outward symptoms, making them especially difficult to diagnose or detect, and thus less likely to be treated (Uhl et al., 2013). Therefore, in order to understand the mechanisms behind TBI and develop proper safety measures, it is essential that accurate instrumentation methods are utilized. The Brain Injury Criterion (BrIC) has been developed and validated to predict brain injuries in combination with the head injury criterion (Takhounts et al., 2011; Takhounts et al., 2013). Being that the validated BrIC is heavily dependent on angular motion, it is expected that the accuracy of any head instrumentation technique should be judged in part by its ability to measure angular motion.

Today there exist sensor configurations that allow for the measurement of three-dimensional kinematics for the purpose of quantifying the severity of an impact. In theory, the most basic would be a six-accelerometer configuration with two accelerometers located along each axis (Becker et al., 1975). While this would require the fewest number of sensors, a system of three nonlinear ordinary differential equations (ODEs) must be solved to calculate angular acceleration and angular velocity, which was found to be inaccurate in high magnitude impacts (Padgaonkar et al., 1975).

A current well-known and popular sensor arrangement is the nine accelerometer array package (NAAP), which is composed of nine accelerometers in a "3-2-2-2" arrangement proposed by Padgaonkar et al., (1975). This nine-accelerometer arrangement contains three central accelerometers situated at a local origin, each oriented in x-, y-, and z-directions, and two accelerometers situated at a fixed radius along each of the three axes, oriented in the two dimensions that exclude the axis dimension. The advantage of this configuration is that angular acceleration can be calculated using algebraic equations rather than a system of differential equations, but a single numerical integration is still required to calculate angular velocity, with a double numerical integration required to calculate rotation. The NAAP has been adapted to the Hybrid III 5th and 50th percentile anthropomorphic test device (ATD) heads, which require a specialized design at additional monetary cost. Furthermore, because the Hybrid III skull is deformed during severe impacts, the rigid body kinematics theory used to calculate angular acceleration using algebraic equations is no longer valid, leading to unreliability and inaccuracy of measurements. In order to avoid issues from skull deformation, instrumentation has to be installed at the center of gravity (CG) of the ATD heads, not peripheral blocks. One possible method that is commonly used involves installation of three accelerometers and three angular rate sensors (ARS). This '3aω' configuration eliminates the need to integrate for angular velocity by incorporating ARS, theoretically eliminating the need for six of the nine accelerometers in the NAAP, while improving accuracy in angular velocity and rotation measurements. This configuration is especially favored in certain biomechanics applications due to its compact size, fewer required sensors that are all mounted at the head CG, and capability and ease of installing in standard non-customized ATD heads. However, using only three accelerometers requires the use of numerical differentiation to determine angular acceleration, rather than algebraic manipulation. This puts the 3aω scheme at a disadvantage to the NAAP when measuring angular acceleration, despite the improvements it provides in measurement of angular velocity and rotation (Kang et al., 2011; Kang et al., 2015).

In order to overcome the numerical disadvantages of the NAAP and 3aω schemes, a '6aω' scheme using six accelerometers and three ARS was proposed and validated (Kang et al., 2011; Kang et al., 2015). In this configuration, numerical differentiation is substituted with algebraic manipulation to measure angular acceleration (maintaining the advantages of NAAP), while numerical integration is not required for angular velocity since it is measured directly by ARS, and only a single numerical integration is required for rotation (the latter two maintaining the advantages of 3aω). Martin et al., (1998) proposed a coplanar scheme using six accelerometers and three ARSs, but it has yet to be evaluated and validated. This scheme is composed of a local origin with three accelerometers and one ARS, and two coplanar arms, one fitted with two accelerometers and one ARS, and the other fitted with one accelerometer and one ARS. This sensor arrangement has the potential to be very practical with respect to measurement of accurate 6-degree-of-freedom (6DOF) kinematics within ATD heads. The main objective of this study was to develop and validate a method of accurately measuring 6DOF kinematics for ATDs using this coplanar 6aω scheme. This instrumentation scheme should allow for angular acceleration to still be calculated from algebraic equations similar to the NAAP, while directly measuring angular velocity and requiring only a single numerical integration for rotation measurement. The novelty and benefit of this configuration lies in its ability to potentially mitigate the accumulation of error associated with numerical methods, such as integration or differentiation, while still being compact, lightweight, easy to install in ATD heads, and with all sensors mounted near the head CG.

METHODS

Coplanar Fixture Design for Hybrid III head

The proposed new fixture design was constrained by essential features such as the correct symmetrical placement of sensors, correct alignment with the Hybrid III 50th percentile male ATD head CG, minimization of mass, easy accessibility, and reduction of noise due to structural vibration. Several designs were proposed, and a modal analysis was conducted on several of them using commercial CAD software. (Solidworks, Dassault Systemes SolidWorks Corporation, Waltham, MA). A fixture that had higher fundamental natural frequency was preferred along with those that were simple to install. The final design was fabricated out of an aluminum alloy and had a mass of 64 grams and a first natural frequency of 4590 Hz (Figure 1). Dimensional information of the proposed coplanar 6aω fixture was compared with the Hybrid III 50th standard head CG mount (Figure 2).

(a) top view (b) oblique view

Figure 1: Coplanar 6aω fixture designed for the Hybrid III 50th percentile male ATD head

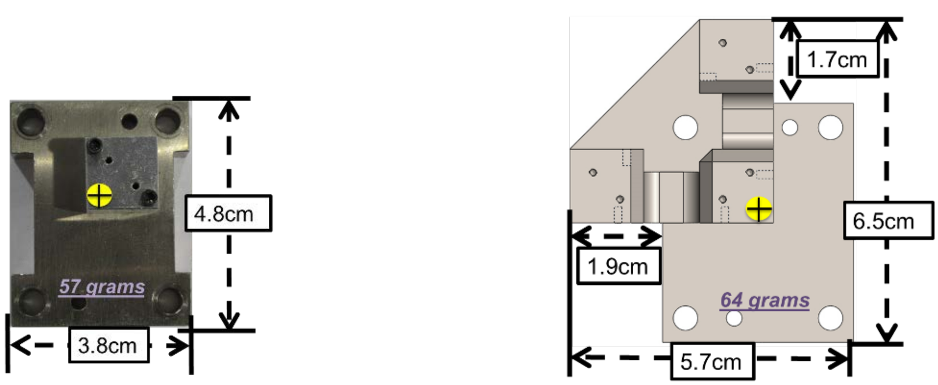

(a) Hybrid III standard head CG mount (b) Proposed coplanar 6aω fixture

Figure 2: Dimensional information (Hybrid III standard vs. proposed coplanar 6aω fixture)

Coplanar 6aω Scheme

The coplanar 6aω scheme (called c6aω hereafter) was implemented as shown in Figure 3. In order to derive algebraic equations for angular acceleration of the c6aω scheme, the acceleration at each corner point (points A and B shown in Figure 3) with respect to the body fixed coordinate system embedded on the coplanar fixture was determined as shown in Eqs (1) – (3).

$$a_{ay'} = a_{0y'} + \omega_{x'}\,\omega_{y'}\rho_{ax'} + \dot{\omega}_{z'}\rho_{ax'} \tag{1}$$

$$a_{az'} = a_{0z'} + \omega_{x'}\,\omega_{z'}\rho_{ax'} - \dot{\omega}_{y'}\rho_{ax'} \tag{2}$$

$$a_{bz'} = a_{0z'} + \omega_{y'}\,\omega_{z'}\rho_{by'} + \dot{\omega}_{x'}\rho_{by'} \tag{3}$$

where,

$\dot{\omega}$: angular acceleration in the body fixed frame

a : acceleration measured from accelerometers at each location

ω : angular velocity measured from ARS

ρ : distance between accelerometers at vertex and accelerometers at points A and B

From using Eqs (1) – (3), angular acceleration can be expressed as:

$$\dot{\omega}_{x'} = -(a_{0z'} - a_{bz'}) / \rho_{by'} - \omega_{y'}\omega_{z'} \tag{4}$$

$$\dot{\omega}_{y'} = (a_{0z'} - a_{az'}) / \rho_{ax'} + \omega_{cx'}\omega_{bz'} \tag{5}$$

$$\dot{\omega}_{z'} = -(a_{0y'} - a_{ay'}) / \rho_{ax'} - \omega_{x'}\omega_{y'} \tag{6}$$

The detailed procedure for deriving the three dimensional kinematic equations with respect to the body fixed frame can be found in a previous study (Kang et al., 2011)

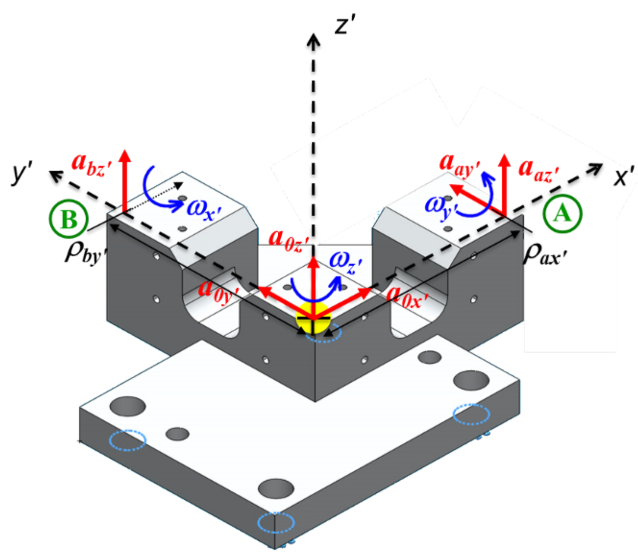

Figure 3: c6aω scheme – body fixed coordinate system embedded on the coplanar fixture

Validation testing setup and instrumentation

The newly designed c6aω fixture was placed at the CG of a Hybrid III 50^{th} percentile ATD head (Figure 4). The c6aω scheme was composed of six accelerometers (Endevco 7264C 2K, San Juan Capistrano, CA) and three ARS (DTS ARS-18K, DTS Technologies, Seal Beach, CA). In addition, nine accelerometers (Endevco 7264C 2K) installed on a tetrahedron fixture (tNAAP), as proposed by Yoganandan et al., (2006), was placed on the posterior surface of the Hybrid III skull cap shown in Figure 5. The c6aω setup also allowed for comparison to the 3aω configuration (called i3aω hereafter) by subsequently treating the c6aω fixture as an i3aω fixture by only using accelerations and angular rates from select sensors. Thus, all three instrumentation methods were used to simultaneously undergo the impact event.

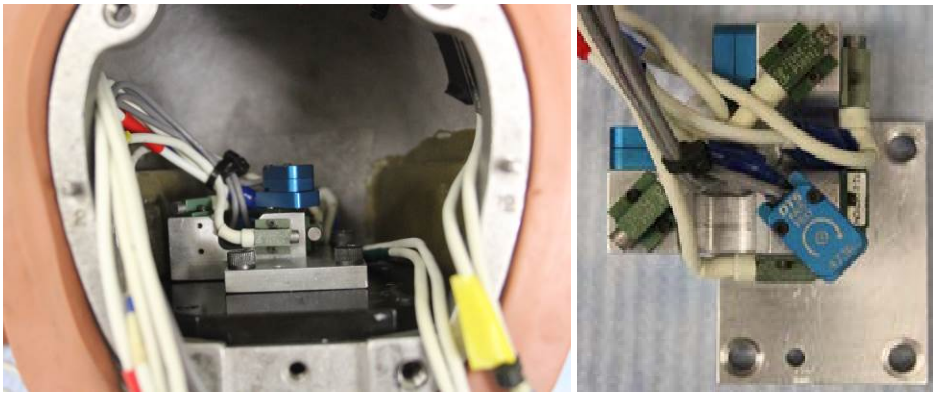

Figure 4: c6aω fixture installed in the Hybrid III 50^{th} percentile male ATD

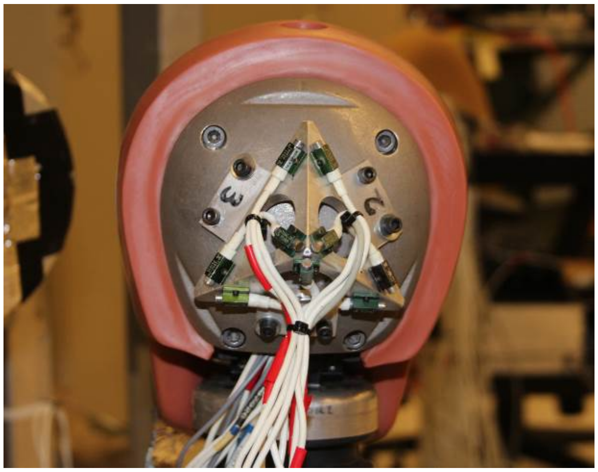

Figure 5: tNAAP configuration installed on the tetrahedron fixture

The head-neck apparatus was impacted at various high speeds and directions by a pneumatic ram (Figure 6). This was done both with the neck secured to a fixed surface as well as sled trials where the apparatus was free to slide along rails in the direction of the ram impact. In each scenario, the impact angles were 30°, 45°, and 60° as shown in Figure 6. For the fixed neck trials, the impact velocities were 1.5m/s, 2.5m/s, and 3m/s, and for the sled trials the impact velocities were 1.5m/s, 2.5m/s, 3m/s, and 3.5m/s. All combinations of neck fixture, angle, and impact speed were repeated three times for a total of 63 tests.

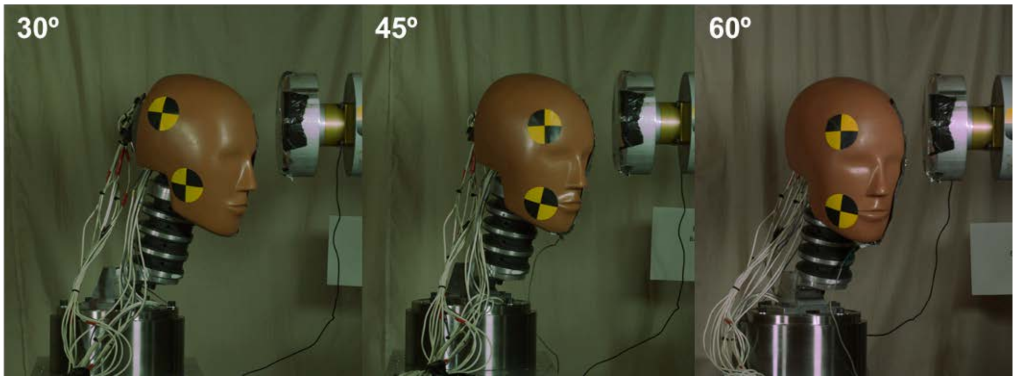

Figure 6: Validation head impact testing setup

Data Analyses

Data was sampled at 20,000 Hz. A 4th-order Butterworth low pass filter in MATLAB (Mathworks, Natick, MA) corresponding to appropriate SAE J211 channel filter classes (CFC) was applied to the data. For the tNAAP and c6aω schemes, the data recorded from the accelerometers and ARS were filtered at 1650 Hz (CFC1000). The angular velocity for the i3aω scheme was first filtered at 1000 Hz (CFC600) and then numerically differentiated to obtain angular acceleration. Angular acceleration for the tNAAP was calculated by employing the procedure proposed by Padgaonkar et al. (1975), while that for the c6aω scheme was determined using Eqs (4) – (6). The kinematic data relative to the body fixed coordinate system on the external fixture was transformed to the body fixed coordinate system on the Hybrid III head using the procedure described in a previous study by Kang (Kang et al., 2011). Origin locations and initial orientation of the body fixed coordinates for both the external tetrahedron fixture and the Hybrid III head were determined by digitizing points on the fixture and the head using a FaroArm device (Faro Arm Technologies, Lake Mary, FL). The normalized root mean square deviation (NRMSD) shown in Eq (7) was used for quantitative evaluation of the proposed scheme. The NRMSD provided an average percent error over time between the tNAAP (i.e. gold standard) and kinematic data (transformed linear acceleration to tetrahedron fixture origin and angular acceleration) obtained from the c6aω and i3aω schemes. In addition to the NRMSD, percent differences of the peak values between the tNAAP and c6aω/i3aω schemes were also calculated since most injury criteria rely upon peak values.

$$NRMSD = \frac{\sqrt{\frac{1}{n}\sum_{i=0}^{n}(Y_i - Y_i')^2}}{Y'_{\max} - Y'_{\min}} \tag{7}$$

where:

- n is the total number of data points
- $Y'max$ and $Y'min$ represent the maximum and minimum values of the gold standard.
- Yi and $Y'i$ are the ith data point obtained from the instrumentation scheme being evaluated and the ith data point obtained from the gold standard, respectively.

RESULTS

In order to provide qualitative analysis for angular acceleration comparison (e.g. c6aω vs. tNAAP and i3aω vs. tNAAP), time history data from a test condition with 45 degree fixed neck at 3 m/s impact are provided in Figure 7. As seen in the figure, angular acceleration from the head impact tests is characterized by very short duration (around 3 ms) and high magnitude (approximately 15000 rad/s^2 in Figure 7c). Qualitatively, c6aω exhibits good agreement with tNAAP results while i3aω produces quite noisy signals.

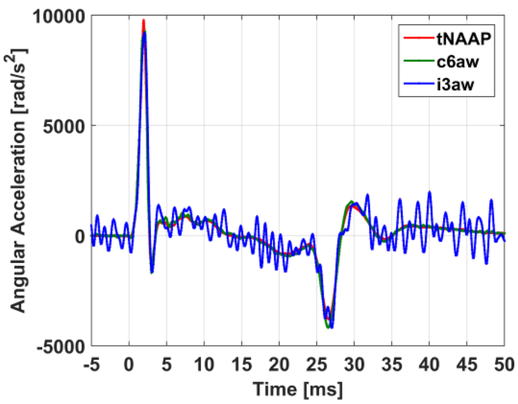

(a) x direction

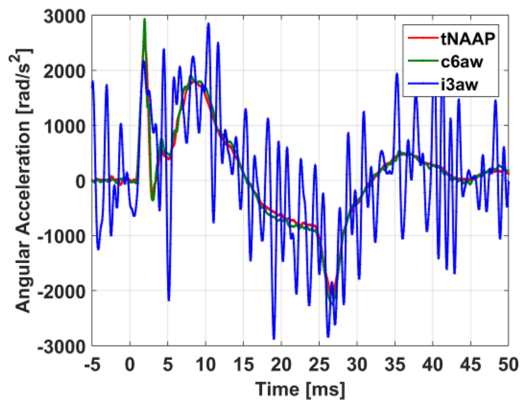

(b) y direction

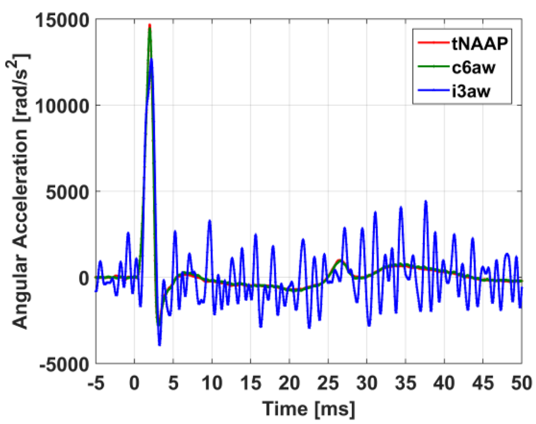

(c) z direction

Figure 7: Time history results for angular acceleration with respect to head body fixed coordinate system
Test condition: 45 degree, fixed neck, and 3 m/s impact speed

For all directions, speeds, and neck fixtures, peak angular acceleration with respect to the x, y and z body fixed head coordinate system for all 63 tests is plotted in Figure 8 (c6aω vs. tNAAP in Figure 8a and i3aω vs. tNAAP in Figure 8b), where the dotted line represents perfect agreement between the instrumentation schemes being compared. The peak angular acceleration determined from the c6aω shows good agreement with those from tNAAP with most of the data being aligned with the dotted line (Figure 8a), while the peak angular acceleration calculated from the i3aω shows more error and variation along the dotted line (Figure 8b). The average NRMSD and peak differences between the calculated angular accelerations were less than 5% between the tNAAP and the c6aω, but greater than 18% for NRMSD and 20% for the peak differences between the tNAAP and i3aω (Figure 9).

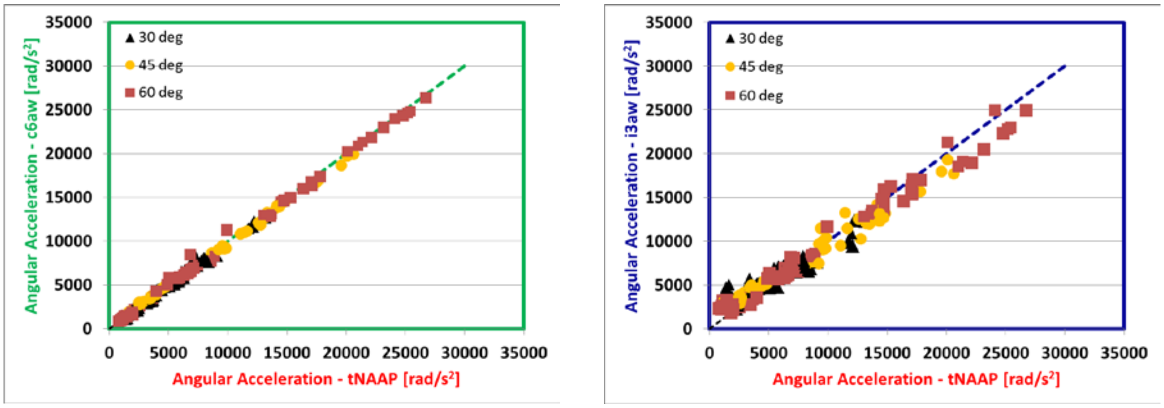

(a) c6aω (algebraic) vs. tNAAP (algebraic)   (b) i3aω (differentiated) vs. tNAAP (algebraic)

Figure 8: Peak angular acceleration calculated from tNAAP (gold standard) vs. c6aω & i3aω for all 63 tests
black triangle: 30 deg impact; orange circle: 45 deg impact; brown square: 60 deg impact
dotted line: perfect agreement (x values equal to y values)

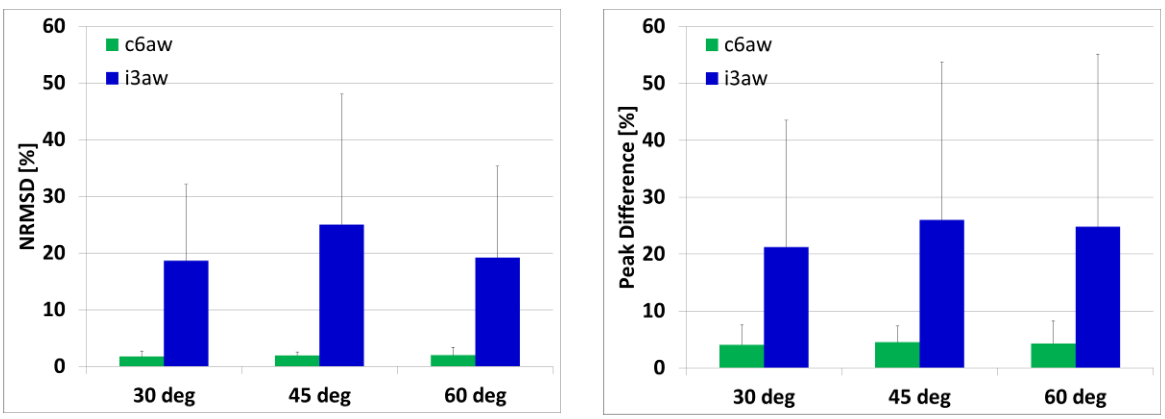

(a) Time history evaluation (NRMSD)
c6aω vs. tNAAP < 5%
i3aω vs. tNAAP >18 %

(b) Peak evaluation
c6aω vs. tNAAP < 5%
i3aω vs. tNAAP >20 %

Figure 9: Average NRMSD and peak differences for angular acceleration in x, y and z components
green bar: c6aω; blue bar: i3aω

Figure 10 shows a comparison of transformed resultant linear acceleration to the origin of the tetrahedron fixture using c6aω and i3aω methods with resultant linear acceleration directly measured by the accelerometers at the origin of the tetrahedron used for tNAAP (the directly measured acceleration was used as the gold standard measure). The c6aω was accurate for these transformed acceleration measurements (Figure 10a), while the i3aω was less accurate, especially for measured accelerations less than 100g shown in Figure 10b. Average NRMSD and peak differences between resultant linear accelerations, transformed from both c6aω and i3aω, as well as directly measured from accelerometers at the origin of tNAAP, were calculated and are shown in Figure 11. Similar to the angular acceleration results, c6aω had NRMSD and peak differences less than 5%, while i3aω had NRMSD over 17% and peak differences over 6%.

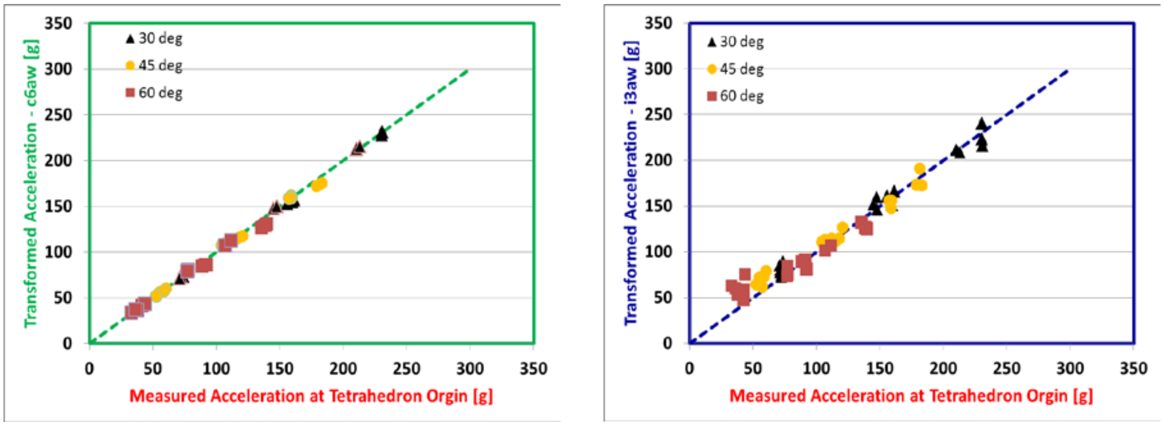

(a) c6aω (transformed) vs. tNAAP (measured) (b) i3aω (transformed) vs. tNAAP (measured)

Figure 10: Peak resultant linear acceleration measured at the origin of tNAAP vs. transformed to the origin using c6aω&i3aω methods for all 63 tests
black triangle: 30 deg impact; orange circle: 45 deg impact; brown square: 60 deg impact
a dotted line: perfect agreement (x values equal to y values)

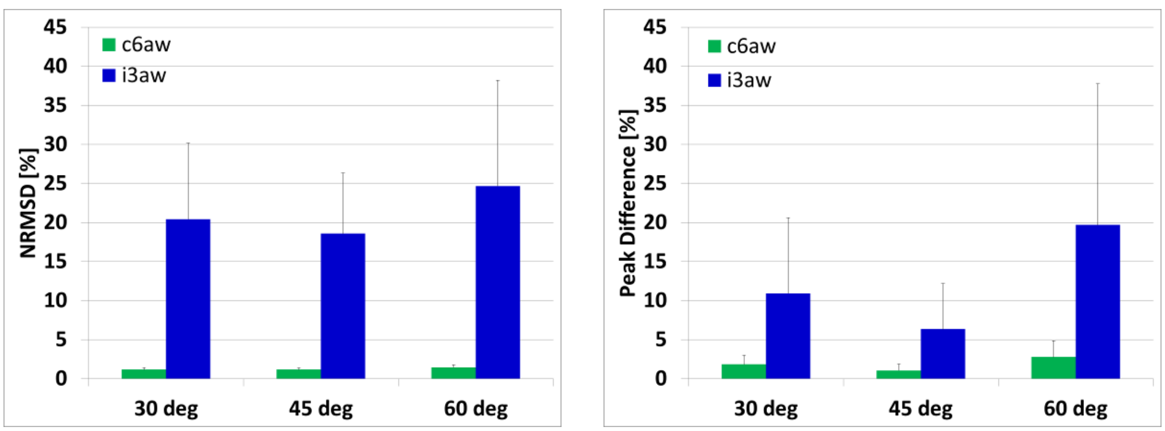

(a) Time history evaluation (NRMSD)
c6aω vs. tNAAP < 5%
i3aω vs. tNAAP >17 %

(b) Peak evaluation
c6aω vs. tNAAP < 5%
i3aω vs. tNAAP >6 %

Figure 11: Average NRMSD and peak differences for resultant linear acceleration at the origin of the tetrahedron fixture
green bar: c6aω; blue bar: i3aω

CONCLUSIONS

TBI is fairly prevalent in car crash scenarios, and an accurate means to predict the likelihood of TBI is predicated on the ability to accurately measure 6DOF kinematics of the head. In this study, a new coplanar configuration using six accelerometers and three ARS was developed and tested for the purposes of measuring 6DOF kinematics in high-magnitude head impacts. The benefits of this configuration are its ability to evade the use of error-producing numerical methods, such as numerical integration and differentiation, often found in traditional sensor configurations. The c6aω configuration was tested in high-magnitude impact scenarios against the traditional tNAAP configuration. The c6aω was able to mimic the accuracy of the NAAP in measuring both linear and angular acceleration, with average NRMSD and peak difference values less than 5% for all 63 trials. The c6aω configuration also has the additional benefit of directly measuring angular velocity, whereas the NAAP requires numerical integration. Likewise for measuring rotation, c6aω only requires single numerical integration whereas NAAP requires double numerical integration. Future plans include refining the design of the current c6aω fixture to even further minimize effects on head CG and mass moment of inertia, as well as other design alterations to make it more universal for other dummy heads. This proposed c6aω is a potential advantageous alternative to the specialized NAAP heads due to its numerical benefits, cost effectiveness, and the elimination of the need to install sensors on the periphery of the skull.

ACKNOWLEDGEMENTS

The authors would like to thank Allison Guettler, Arri Willis, Alex Redrow, and Dr. Kyle Icke from the injury biomechanics research center for their considerable support during test days.

REFERENCES

BECKER, E., and WILLEMS, G. (1975). An experimentally validated 3-D inertial tracking package for application in biodynamic research. J. Stapp Car Crash, 19, pp. 899–930.

FAUL, M., XU, L., WALD, M. M., and CORONADO, V. G. (2010). Traumatic brain injury in the United States. Atlanta, GA: Centers for Disease Control and Prevention, National Center for Injury Prevention and Control.

KANG, Y. S., MOORHOUSE, K., and BOLTE, J. H. (2011). Measurement of six degrees of freedom head kinematics in impact conditions employing six accelerometers and three angular rate sensors (6aω configuration). J. biomechanical engineering, 133(11), 111007.

KANG, Y. S., MOORHOUSE, K., and BOLTE IV, J. H. (2015). Instrumentation Technique for Measuring Six Degrees of Freedom Head Kinematics in Impact Conditions using Six-Accelerometers and Three-Angular Rate Sensors (6aω Configuration) on a Lightweight Tetrahedron Fixture. Proc. 24th International Technical Conference on the Enhanced Safety of Vehicles (ESV) (No. 15-0288).

MARTIN, P. G., HALL, G. W., CRANDALL, J. R., and PILKEY, W. D. (1998). Measuring the acceleration of a rigid body. Shock and Vibration, 5(4), 211-224.

PADGAONKAR, A. J., KRIEGER, K. W., and KING, A. I. (1975). Measurement of angular acceleration of a rigid body using linear accelerometers. J. Applied Mechanics, 42(3), 552-556.

TAKHOUNTS, E. G., HASIJA, V., RIDELLA, S. A., ROWSON, S., and DUMA, S. M. (2011). Kinematic rotational brain injury criterion (BRIC). In Proceedings of the 22nd Enhanced Safety of Vehicles Conference. Paper (No. 11-0263).

TAKHOUNTS, E. G., CRAIG, M. J., MOORHOUSE, K., MCFADDEN, J., and HASIJA, V. (2013). Development of brain injury criteria (BrIC). Stapp car crash journal, 57, 243.

UHL, R. L., ROSENBAUM, A. J., CZAJKA, C., MULLIGAN, M., and KING, C. (2013). Minor traumatic brain injury: a primer for the orthopaedic surgeon. J. the American Academy of Orthopaedic Surgeons, 21(10), 624-631.

YOGANANDAN, N., ZHANG, J., PINTAR, F. A., and LIU, Y. K. (2006). Lightweight low-profile nine-accelerometer package to obtain head angular accelerations in short-duration impacts. J. Biomechanics, 39(7), 1347-1354.

All Authors full name, address and E-mail

Yun-Seok Kang
Injury Biomechanics Research Center
333 West 10th Ave, 2063 Graves Hall
Columbus, OH 43210
Phone: 614-366-7584; Fax: 614-292-7659
Yunseok.kang@osumc.edu

Sam Goldman
Injury Biomechanics Research Center
333 West 10th Ave, 2063 Graves Hall
Columbus, OH 43210
Phone: 614-292-4448; Fax: 614-292-7659
Goldman.115@buckeyemail.osu.edu

Kevin Moorhouse
NHTSA/VRTC
P.O. Box B-37, 10820 State Route 347
East Liberty, OH 43319
Phone: 937-66-3283; Fax: 937- 666-3590
Kevin.Moorhouse@dot.gov

John H. Bolte IV
Injury Biomechanics Research Center
333 West 10th Ave, 2063 Graves Hall
Columbus, OH 43210
Phone: 614-688-4015; Fax: 614-292-7659
John.Bolte@osumc.edu